**Appendix for:**

# PIWI proteins tether piRNA biogenesis machinery to mitochondria in mice

Jie Gao, Canmei Chen, Guanyi Shang, Wenyang Yu, Ting Zhao, Yunfang Zhang, Chen Chen and Deqiang Ding

* Correspondence: dingdeqiang@tongji.edu.cn

**Table of Contents:**

Appendix Figure S1. GPAT2 and mitoPLD could not recruit piRNA pathway proteins to mitochondria.....2

Appendix Figure S2. TDRD1 is required for IMC assembly and pachytene piRNA biogenesis in adult testes.....3-4

Appendix Table S1. Constructs used in this study.....5-7

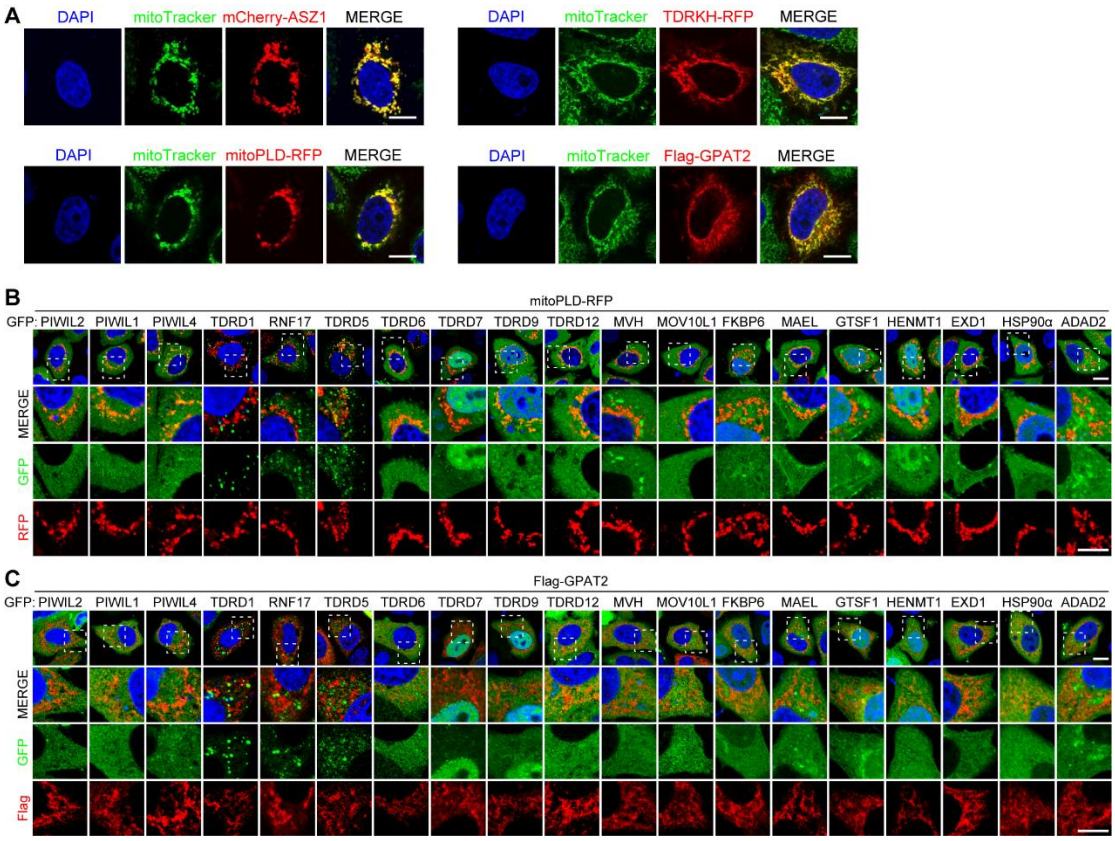


**Appendix Figure S1. GPAT2 and mitoPLD could not recruit piRNA pathway proteins to mitochondria.**

**A** HeLa cells were transfected with indicated constructs. Transfected cells were stained with Mitotracker to label mitochondria. Immunostaining was performed using Flag antibody. Scale bars, 10 μm.

**B,C** Images of HeLa cells transfected with indicated plasmids. Dotted boxes indicate the zoomed-in areas showing in below. Scale bars, 10 μm.

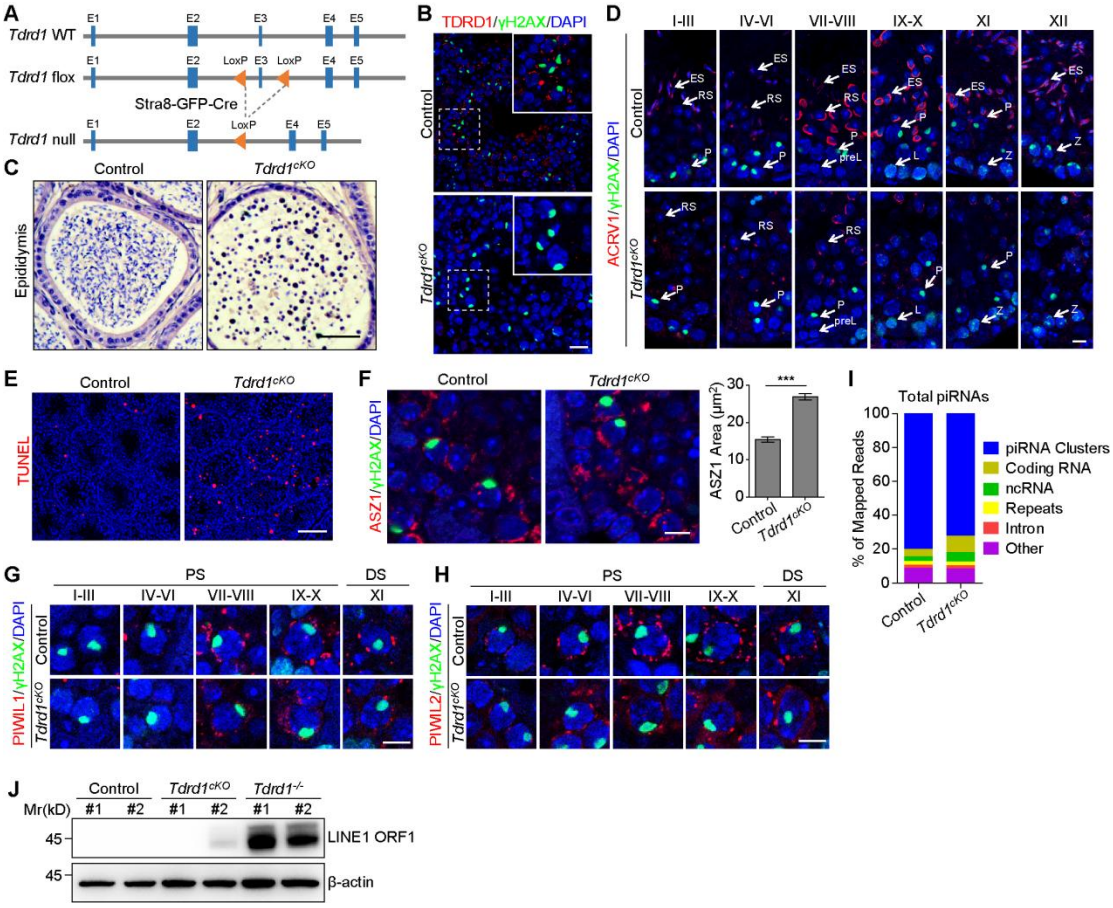


**Appendix Figure S2. TDRD1 is required for IMC assembly and pachytene piRNA biogenesis in adult testes.**

**A** A schematic diagram showing the gene targeting strategy for the generation of a *Tdrd1* conditional allele. Cre-mediated deletion removed the exon 3 of *Tdrd1* and generated a protein null allele.

**B** Co-immunostaining of TDRD1 and γH2AX on control and *Tdrd1*$^{cKO}$ adult testes. Scale bars, 20 μm.

**C** H&E staining on epididymis from adult mice. Scale bars, 50 μm.

**D** Co-immunostaining of ACRV1 and γH2AX on adult mouse testes. preL, prelepotene; L, lepotene; Z, zygotene; P, pachytene; D, diplotene; M, metaphase; RS, round spermatid; ES, elongated spermatid; Scale bars, 10 μm.

**E** TUNEL assays on adult testes. Scale bars, 100 μm.

**F** Co-immunostaining of ASZ1 and γH2AX on adult testes. Scale bars, 10 μm. Mitochondrial areas corresponding to ASZ1 immunostaining signal in each pachytene spermatocytes (VII-VIII) are shown on the right. ($n = 50$; ***$p < 0.001$).

**G,H** Co-immunostaining of PIWIL1 and γH2AX (G) or PIWIL2 and γH2AX (H) on adult testes. PS, pachytene spermatocytes; DS, diplotene spermatocytes; Scale

bars, 10 μm. The developmental stages of germ cells were distinguished according to γH2AX and DAPI staining.

**I** Genomic annotation of piRNAs from control and *Tdrd1*$^{cKO}$ adult testes. Data are representative of 3 biological replicates.

**J** WB of LINE1 ORF1 in adult testes. β-actin served as a control.

Data information: In (F), data are presented as mean ± s.e.m and *p* values were calculated using Student's t-test (***$p < 0.001$). $p = 8.6541E\text{-}13$ (F).

## Appendix Table S1. Constructs used in this study.

| Construct | Source | Uniprot ID | Insert Sequence Region | Backbone |
|---|---|---|---|---|
| Flag | (Gao *et al*, 2024) | N/A | N/A | pcDNA3-Flag |
| Flag-TDRD1 | (Gao *et al.*, 2024) | Q99MV1 | 1-1172 | pcDNA3-Flag |
| Flag-TDRD1-3GS | (Gao *et al.*, 2024) | Q99MV1 | 1149-1154: ILLFLL→GSGSGS | pcDNA3-Flag |
| Flag-TDRKH | (Ding *et al*, 2019) | Q80VL1 | 1-560 | pcDNA3-Flag |
| Flag-mitoPLD | This paper | Q5SWZ9 | 1-221 | pcDNA3-Flag |
| Flag-GPAT2 | This paper | Q14DK4 | 1-801 | pcDNA3-Flag |
| Flag-PNLDC1 | (Ding *et al.*, 2019) | B2RXZ1 | 1-531 | pcDNA3-Flag |
| Flag-ASZ1 | (Ding *et al.*, 2019) | Q8VD46 | 1-475 | pcDNA3-Flag |
| Flag-PIWIL2 | This paper | Q8CDG1 | 1-971 | pcDNA3-Flag |
| Flag-PIWIL2-RK | This paper | Q8CDG1 | 9/39/45/74/95/100 /144/156/163 R→K | pcDNA3-Flag |
| Flag-PIWIL2-Δ1-200 | This paper | Q8CDG1 | 201-971 | pcDNA3-Flag |
| Flag-PIWIL2-Δ201-600 | This paper | Q8CDG1 | 1-200; 601-971 | pcDNA3-Flag |
| Flag-PIWIL2-Δ601-971 | This paper | Q8CDG1 | 1-600 | pcDNA3-Flag |
| Flag-PIWIL2-(1-200) | This paper | Q8CDG1 | 1-200 | pcDNA3-Flag |
| Flag-PIWIL2-(201-600) | This paper | Q8CDG1 | 201-600 | pcDNA3-Flag |
| Flag-PIWIL2-(601-971) | This paper | Q8CDG1 | 601-971 | pcDNA3-Flag |
| Flag-ASZ1 | This paper | Q8VD46 | 1-475 | pcDNA3-Flag |
| Flag-ASZ1-Δ1-32 | This paper | Q8VD46 | 33-475 | pcDNA3-Flag |
| Flag-MOV10L1 | This paper | Q99MV5 | 1-1187 | pcDNA3-Flag |
| Flag-TDRD5 | This paper | Q5VCS6 | 1-1040 | pcDNA3-Flag |
| Flag-PIWIL1 | (Wei *et al*, 2023) | Q9JMB7 | 1-862 | pcDNA3-Flag |
| Flag-PIWIL1-RK | (Wei *et al.*, 2023) | Q9JMB7 | 4/6/8/10/12/14/49/51/53/80/83/84/85 R→K | pcDNA3-Flag |
| Flag-PIWIL1-Δ1-278 | This paper | Q9JMB7 | 279-862 | pcDNA3-Flag |
| Flag-PIWIL1-Δ279-555 | This paper | Q9JMB7 | 1-278; 556-862 | pcDNA3-Flag |
| Flag-PIWIL1-Δ556-862 | This paper | Q9JMB7 | 1-555 | pcDNA3-Flag |
| HA | This paper | N/A | N/A | pcDNA3-HA |
| HA-TDRD1 | (Gao *et al.*, 2024) | Q99MV1 | 1-1172 | pcDNA3-HA |
| HA-PIWIL2 | (Gao *et al.*, 2024) | Q8CDG1 | 1-971 | pcDNA3-HA |
| HA-PIWIL2-RK | This paper | Q8CDG1 | 9/39/45/74/95/100 | pcDNA3-HA |

| | | | | |
|---|---|---|---|---|
| | | | /144/156/163 R→K | |
| HA-PIWIL1 | This paper | Q9JMB7 | 1-862 | pcDNA3-HA |
| HA-PIWIL1-(1-278) | This paper | Q9JMB7 | 1-278 | pcDNA3-HA |
| HA-PIWIL1-(279-555) | This paper | Q9JMB7 | 279-555 | pcDNA3-HA |
| HA-PIWIL1-(556-862) | This paper | Q9JMB7 | 556-862 | pcDNA3-HA |
| mCherry-ASZ1 | This paper | Q8VD46 | 1-475 | pcDNA3-mCherry |
| mCherry-TDRD1 | This paper | Q99MV1 | 1-1172 | pcDNA3-mCherry |
| RFP-ASZ1 | This paper | Q8VD46 | 1-475 | pcDNA3-RFP |
| TDRKH-RFP | (Ding *et al.*, 2019) | Q80VL1 | 1-560 | pRFP-N1 |
| mitoPLD-RFP | This paper | Q5SWZ9 | 1-221 | pRFP-N1 |
| TDRKH-GFP | (Gao *et al.*, 2024) | Q80VL1 | 1-560 | pEGFP-N1 |
| mitoPLD-GFP | (Gao *et al.*, 2024) | Q5SWZ9 | 1-221 | pEGFP-N1 |
| GPAT2-GFP | (Gao *et al.*, 2024) | Q14DK4 | 1-801 | pEGFP-N1 |
| GFP-ASZ1 | (Gao *et al.*, 2024) | Q8VD46 | 1-475 | pEGFP-C1 |
| GFP-ASZ1-Δ1-32 | This paper | Q8VD46 | 33-475 | pEGFP-C1 |
| GFP-PNLDC1 | (Gao *et al.*, 2024) | B2RXZ1 | 1-531 | pEGFP-C1 |
| GFP-PIWIL2 | (Gao *et al.*, 2024) | Q8CDG1 | 1-971 | pEGFP-C1 |
| GFP-PIWIL2-TM | (Gao *et al.*, 2024) | Q8CDG1<br>Q8VD46 | 1-971; 426-475 | pEGFP-C1 |
| GFP-PIWIL1 | (Ding *et al.*, 2019) | Q9JMB7 | 1-862 | pEGFP-C1 |
| GFP-PIWIL1-TM | This paper | Q9JMB7<br>Q8VD46 | 1-862; 426-475 | pEGFP-C1 |
| GFP-PIWIL4 | (Ding *et al.*, 2019) | Q8CGT6 | 1-848 | pEGFP-C1 |
| GFP-TDRD1 | (Gao *et al.*, 2024) | Q99MV1 | 1-1172 | pEGFP-C1 |
| GFP-TDRD1-3GS | (Gao *et al.*, 2024) | Q99MV1 | 1149-1154:<br>ILLFLL→GSGSGS | pEGFP-C1 |
| GFP-RNF17 | (Wei *et al.*, 2023) | Q99MV7 | 1-1640 | pEGFP-C1 |
| GFP-TDRD5 | (Ding *et al*, 2020) | Q5VCS6 | 1-1040 | pEGFP-C1 |
| GFP-TDRD6 | (Wei *et al.*, 2023) | P61407 | 1-2134 | pEGFP-C1 |
| GFP-TDRD7 | This paper | Q8K1H1 | 1-1086 | pEGFP-C1 |

| | | | | |
|---|---|---|---|---|
| GFP-TDRD9 | This paper | Q14BI7 | 1-1383 | pEGFP-C1 |
| GFP-TDRD12 | This paper | Q9CWU0 | 1-1277 | pEGFP-C1 |
| GFP-MVH | This paper | Q61496 | 1-702 | pEGFP-C1 |
| GFP-MOV10L1 | (Wei *et al.*, 2023) | Q99MV5 | 1-1187 | pEGFP-C1 |
| GFP-FKBP6 | This paper | Q91XW8 | 1-327 | pEGFP-C1 |
| GFP-MAEL | This paper | Q8BVN9 | 1-434 | pEGFP-C1 |
| GFP-GTSF1 | This paper | Q9DAN6 | 1-167 | pEGFP-C1 |
| GFP-HENMT1 | This paper | Q8CAE2 | 1-395 | pEGFP-C1 |
| GFP-EXD1 | This paper | Q8CDF7 | 1-570 | pEGFP-C1 |
| GFP-HSP90α | This paper | P07901 | 1-733 | pEGFP-C1 |
| GFP-ADAD2 | This paper | Q9D5P4 | 1-561 | pEGFP-C1 |

## Reference


Ding D, Liu J, Dong K, Melnick AF, Latham KE, Chen C (2019) Mitochondrial membrane-based initial separation of MIWI and MILI functions during pachytene piRNA biogenesis. *Nucleic Acids Res* 47: 2594-2608

Ding D, Wei C, Dong K, Liu J, Stanton A, Xu C, Min J, Hu J, Chen C (2020) LOTUS domain is a novel class of G-rich and G-quadruplex RNA binding domain. *Nucleic Acids Res* 48: 9262-9272

Gao J, Jing J, Shang G, Chen C, Duan M, Yu W, Wang K, Luo J, Song M, Chen K et al (2024) TDRD1 phase separation drives intermitochondrial cement assembly to promote piRNA biogenesis and fertility. *Dev Cell* 59: 2704-2718.e2706

Wei C, Jing J, Yan X, Mann JM, Geng R, Xie H, Demireva EY, Hess RA, Ding D, Chen C (2023) MIWI N-terminal RG motif promotes efficient pachytene piRNA production and spermatogenesis independent of LINE1 transposon silencing. *PLoS Genet* 19: e1011031